SPANDIDOS PUBLICATIONS

ONCOLOGY REPORTS 41: 961-972, 2019

Functional analysis of protein disulfide isomerase P5 in glioblastoma cells as a novel anticancer target

TOMOHISA HORIBE, AYA TORISAWA, YOSHIE MASUDA and KOJI KAWAKAMI

Department of Pharmacoepidemiology, Graduate School of Medicine and Public Health, Kyoto University, Kyoto 606-8501, Japan

Received May 22, 2018; Accepted October 9, 2018

DOI: 10.3892/or.2018.6868

Abstract. P5, which is a member of the protein disulfide isomerase family, possesses isomerase and chaperone activity *in vitro*; however, the physiological functions of this enzyme in cells remain unclear. To understand the important roles of P5 in cancer cells, the present study examined its expression on the surface of normal and cancer cell lines by flow cytometry using an affinity-purified anti-P5 antibody labeled with 6-(fluorescein-5-carboxamido) hexanoic acid succinimidyl ester. P5 expression was increased on the surface of various cancer cell lines, including leukemia cells, and glioblastoma, breast, colon, ovarian and uterine cervical cancer cells, compared with normal cells. However, P5 was constantly expressed within both normal and cancer cell lysates, and its total expression levels were not significantly different between the cells. P5 knockdown in glioblastoma cells by small interfering RNA affected Bip promoter activation during cancer cell growth, and significantly inhibited cancer cell growth and migration. Immunoprecipitation using an anti-P5 antibody in cancer and normal cells demonstrated that vimentin was bound to P5, predominantly in U251 glioblastoma cells. P5 knockdown in glioblastoma cells did not affect the protein expression levels of vimentin; however, it did affect the expression of numerous epithelial-mesenchymal transition markers, including Snail and Slug. These results suggested that P5 may serve an important role in cancer cell growth, and may be considered an attractive and potent target for the treatment of glioblastoma.

Correspondence to: Dr Tomohisa Horibe, Department of Pharmacoepidemiology, Graduate School of Medicine and Public Health, Kyoto University, G Building, Yoshida Konoe-cho, Sakyo-ku, Kyoto 606-8501, Japan
E-mail: horibe.tomohisa.5z@kyoto-u.ac.jp

Key words: protein disulfide isomerase, P5, cancer cells, bioluminescence imaging, molecular targeted therapy

Introduction

Protein disulfide isomerase (PDI) is a member of the thioredoxin superfamily that catalyzes the oxidation, reduction and isomerization of protein disulfide bonds via two redox active sites consisting of -Cys-Gly-His-Cys- (CXXC motif), which are located in two thioredoxin fold domains. The functions of PDI are important for the correct folding of newly synthesized polypeptides in the endoplasmic reticulum (ER) (1). At present, 21 genes have been classified as encoding PDI and associated proteins, and these PDI family proteins have thioredoxin-like folds or thioredoxin-like active sequences, with a CXXC motif in their amino acid sequences (2). PDI P5 (P5, also known as PDIA6) contains two redox active -Cys-Gly-His-Cys- sequences, which are indispensable for the isomerase activity of this enzyme. In addition, it has chaperone activity, although the activities of P5 are weaker than those of PDI (3). Currently, the detailed physiological roles of P5 in cells are unknown. It was previously reported that P5 is associated with major histocompatibility complex class I polypeptide-related sequence A (MICA) on the surface of cancer cells and is required for the secretion of soluble MICA from cancer cells, which promotes immune evasion by these cells (4). Furthermore, P5 is localized not only to the ER but also to the mitochondria, and MTS-P5 cells, in which P5 is stably expressed in the mitochondria of Saos-2 cells, are resistant to H_2O_2- or rotenone-induced cell death (5,6). These findings suggested that there are still unidentified roles for P5 in cells. Previous studies regarding PDIs revealed important roles for these enzymes in cancer cells and suggested that they may be promising targets for cancer therapy (7-10); however, the functional roles of P5 and the significance of targeting this enzyme in cancer cells are currently unclear.

In order to regulate the activity of P5 in cancer cells, our previous study screened for specific inhibitors of P5 using a chemical compound library and revealed that anacardic acid is able to inhibit the reductase activity of P5, but does not inhibit the activity of other PDI family proteins, such as PDI, ERp57 or thioredoxin (11). Furthermore, anacardic acid is able to decrease the secretion of soluble MICA from cancer cells (11). These results suggested that targeting P5 on cancer cells may lead to the identification of novel types of cancer chemotherapy; however, further investigation into the detailed functional roles of P5 in cancer cells is required.

The present study detected the expression levels of P5 on the surface of several normal and cancer cell lines. The results revealed that P5 expression was increased on the surface of cancer cells compared with normal cell lines. Furthermore, the effects of P5 knockdown on cancer cells were determined with regards to Bip promoter activation, cell growth and migration. Screening for P5-specific binding proteins was conducted in cancer cells compared with normal cells, and vimentin was identified as one such protein. Finally, the effects of P5 knockdown on cancer cells were determined with regards to the expression levels of vimentin and epithelial-mesenchymal transition (EMT) markers. Bip promoter activation and cell morphology were assessed simultaneously at the single-cell level using a real-time monitoring method, which utilizes bioluminescence and fluorescence. The present study also discussed the potency of targeting P5 in cancer cells as a novel type of cancer treatment.

Materials and methods

Materials. The affinity-purified rabbit anti-P5 antibody used in this study was kindly provided by Dr T. Komiya (Nagahama Institute of Bio-Science and Technology, Nagahama, Japan) (6). The rabbit anti-PDI polyclonal antibody was prepared as previously described (12). Protein G PLUS-agarose was purchased from Santa Cruz Biotechnology, Inc. (Dallas, TX, USA). Recombinant human vimentin protein was purchased from PeproTech, Inc. (Rocky Hill, NJ, USA). Anacardic acid, ribostamycin, bovine serum albumin (BSA) and purified PDI were purchased from Sigma-Aldrich (Merck KGaA, Darmstadt, Germany). Temozolomide (TMZ) was purchased from LKT Laboratories, Inc. (St. Paul, MN, USA). Pre-stained protein markers for SDS-PAGE and thapsigargin (Tg) were purchased from Nacalai Tesque, Inc. (Kyoto, Japan). The other reagents were mostly obtained from Nacalai Tesque, Inc. All reagents used were of research grade.

Cells and cell culture. The normal and cancer cell lines used in the present study are presented in Table I. A172, SNB19, T98G, BT20, MDA-MB-231, T47D, H322, H460, H526, Panc-1, SU86.86, Caki-1, LNCaP, PA-1, HeLa and WI38 cell lines were obtained from the American Type Culture Collection (Manassas, VA, USA). BxPC3, HCT116, SK-OV-3 and OE19 cell lines were obtained from the European Collection of Authenticated Cell Cultures (Salisbury, UK). HepG2, HuCCT-1, KMRC-1, DLD-1, LoVo, SW837, PC-3, U937, HL-60, K562 and THP-1 cell lines were obtained from Health Science Research Resources Bank (Osaka, Japan). SW48 and SW480 cells were purchased from DS Pharma Biomedical Co., Ltd. (Osaka, Japan). Astrocytes (ACBRI371), pancreatic epithelial (PE) cells (ACBRI515), and hepatocytes (ACBRI3716) were purchased from Cell Systems (Kirkland, WA, USA) via DS Pharma Biomedical Co., Ltd. U251 and 293T cell lines were obtained from the National Cancer Institute, Frederick Cancer Research Facility, Division of Cancer Treatment Tumor Repository Program (Frederick, MD, USA) and RIKEN BioResource Center (Tsukuba, Japan), respectively. The ML-RCC cell line was kindly provided by Dr R. Puri (Center for Biological Evaluation, Food and Drug Administration, Silver Spring, MD, USA); the cell line was established as previously described (13). The cells were cultured in RPMI-1640 (Nacalai Tesque, Inc.) (U251, A172, SNB19, BT20, MDA-MB-231, T47D, H322, H460, H526, BxPC3, SU86.86, HuCCT-1, ML-RCC, DLD-1, SW837, LNCap, OE19, U937, HL-60, K562 and THP-1), McCoy's 5A (Thermo Fisher Scientific, Inc., Waltham, MA, USA) (Caki-1, HCT-116 and SK-OV-3), Dulbecco's modified Eagle's medium (DMEM) (Nacalai Tesque, Inc.) (Panc-1, KMRC-1, HeLa and 293T), MEM (Nacalai Tesque, Inc.) (T98G, HepG2, PC-3, PA-1 and WI38), DMEM/F12 (Nacalai Tesque, Inc.) (LoVo, SW48 and SW480) or Complete medium kit (cat no. 4Z0-500-R; Cell Systems) (astrocytes, PE cells and hepatocytes) containing 10% fetal bovine serum (cat no. 172012-500ML; Sigma-Aldrich; Merck KGaA), 100 μg/ml penicillin and 100 μg/ml streptomycin at 37˚C in an atmosphere containing 5% CO_2 and 95% ambient air. All of the cell lines were used for flow cytometry and western blotting to assess the expression levels of P5. U251/Luc, SNB19, PE and astrocytes were used for the cell growth assay post-transfection with siRNA. U251, PE, BT20, H322, DLD-1, PA-1 and U937 cells were used for immunoprecipitation. U251/Luc cells were used for all other experiments described in this study.

Table I. Normal and cancer cell lines used to analyze the expression levels of P5.

Organ	Cell lines
Cancer	
Brain	U251, A172, SNB19, T98G
Breast	BT20, MDA-MB-231, T47D
Lung	H322, H460, H526
Pancreas	BxPC3, Panc-1, SU86.86
Liver	HepG2, HuCCT-1
Kidney	Caki-1, KMRC-1, ML-RCC
Colon	DLD-1, HCT116, LoVo, SW48, SW480
Rectum	SW837
Prostate	LNCaP, PC-3
Ovary	PA-1, SK-OV-3
Uterine cervix	HeLa
Esophagus	OE19
Blood	U937, HL-60, K562, THP-1
Normal	
Brain	Astrocyte
Lung	WI38
Pancreas	Pancreatic epithelial cells
Liver	Hepatocyte cells
Kidney	293T

Expression and purification of human P5. Recombinant human P5 protein was purified using a Ni^{2+}-chelating Resin Column (GE Healthcare Bio-Sciences, Pittsburgh, PA, USA), as previously described (11,12).

Specificity of the anti-P5 antibody to P5 protein. PDI, P5 and BSA proteins (1.6 μg) were separated by 12.5% SDS-PAGE,

and western blotting was performed using rabbit anti-PDI (1:6,000) or anti-P5 (1:6,000) antibodies as primary antibodies, and horseradish peroxidase-conjugated donkey anti-rabbit immunoglobulin G (IgG) (1:2,000; cat. no. NA934-1ML; GE Healthcare Bio-Sciences) as a secondary antibody. The staining of gel and membranes following SDS-PAGE and western blotting was performed using Coomassie Brilliant Blue (Nacalai Tesque, Inc.) and the Peroxidase Stain DAB kit (Nacalai Tesque, Inc.), respectively.

Western blotting. Western blotting was conducted as previously described (14). Briefly, total protein extracts were prepared from cells lysed with reporter lysis buffer (Promega Corporation, Madison, WI, USA). Subsequently, total protein concentration was quantified by measuring the absorbance at 280 nm using a NanoDrop 1000 spectrophotometer (NanoDrop; Thermo Fisher Scientific, Inc., Wilmington, DE, USA). Proteins (20 μg/lane) were separated by 12.5% SDS-PAGE and transferred to nitrocellulose membranes using the iBlot system (Thermo Fisher Scientific, Inc.), according to the manufacturer's protocol. The membranes were blocked with 5% skim milk (w/v) in PBS for 90 min at room temperature, after which, the membranes were probed with anti-P5 (1:6,000), anti-Bip (1:500; cat. no. MAB4846; R&D Systems, Inc. Minneapolis, MN, USA), anti-vimentin (1:800; cat. no. ab20346; Abcam, Cambridge, UK) or anti-β-actin (1:4,000; cat no. A5316-.2ML; Sigma-Aldrich; Merck KGaA) as primary antibodies overnight at 4˚C, and with a horseradish peroxidase-conjugated donkey anti-rabbit IgG (1:2,000; cat. no. NA934-1ML; GE Healthcare Bio-Sciences) or sheep anti-mouse IgG (1:2,000; cat. no. NA931-1ML; GE Healthcare Bio-Sciences) secondary antibody for 3 h at room temperature. The blots were then analyzed with Chemi-Lumi One Super reagent (Nacalai Tesque, Inc.) using a LAS-3000 LuminoImage analyzer (Fujifilm, Tokyo, Japan). Densitometric analysis of the bands obtained from western blotting was performed using Multi Gauge software V3.0 (Fujifilm).

Flow cytometry. Flow cytometry was performed as previously described (15). Briefly, the affinity-purified rabbit anti-P5 antibody was labeled with 6-(fluorescein-5-carboxamido) hexanoic acid succinimidyl ester (FAM-X) using a FAM-X labeling kit (KPL, Inc., Gaithersburg, MD, USA), according to the manufacturer's protocol. Subsequently, $1.0x10^5$ normal or cancer cells were incubated with the labeled antibody for 2 h at room temperature. After incubation, the cells were washed twice with PBS and flow cytometry was performed using FACSCalibur (BD Biosciences, San Jose, CA, USA). The data were analyzed using CellQuest software version 6.0 (BD Biosciences).

Small interfering (si)RNA transfection. Stealth RNA interference (RNAi) duplexes, negative control medium GC (cat. no. 12935300; Thermo Fisher Scientific, Inc.) and P5 siRNA (5'-CCAUAUCCUUGAUACUGGAGCUGCA-3' and 5'-UGCAGCUCCAGUAUCAAGGAUAUGG-3') (Invitrogen; Thermo Fisher Scientific, Inc.) were used for P5 knockdown experiments, as previously described (16). Briefly, U251/Luc, SNB19, PE cells and astrocytes were grown to 40-50% confluence on a 6-well plate or 35 mm glass-bottomed dish; the cells were and transfected with 0.125 or 0.25 μM siRNA in incomplete medium without FBS, penicillin and streptomycin. siRNA transfection was performed using Lipofectamine RNAiMAX (Invitrogen; Thermo Fisher Scientific, Inc.), according to the manufacturer's protocol (6,16). After transfection, cells were kept at 37˚C for 3 h, and medium was replaced with complete medium. A total of 24 h post-transfection, bioluminescence imaging was performed, and 48 or 72 h post-transfection, cell samples were prepared for western blotting or reverse transcription-polymerase chain reaction (RT-PCR). A total of 72 h post-transfection, cells were seeded in 96-well plates for cell growth and migration assays.

Cell growth, viability and migration assays. Cell growth was assessed using the WST-8 assay, as previously described (15). Briefly, cells were seeded in 96-well plates at a concentration of 3,000 cells/well, and the number of living cells was measured using Cell Count Reagent SF (Nacalai Tesque, Inc.). Absorbance was measured at a wavelength of 450 nm using a microplate reader (GE Healthcare Bio-Sciences). Cell viability was also assessed using the WST-8-assay, as previously described (15). Briefly, U251/Luc cells were seeded in 96-well plates as aforementioned, and were treated with various concentrations (0, 25, 50, 100 and 200 μM) of TMZ in the presence or absence of 25 μM anacardic acid, 1 mM ribostamycin, or a combination of these compounds. Cell viability was calculated after 48 h; the viability of untreated control cells was set to 100%. Cell migration was assessed using an Oris™ Cell migration assay (Platypus Technologies, LLC, Madison, WI, USA), according to the manufacturer's protocol.

Immunoprecipitation. Immunoprecipitation was performed using an anti-P5 antibody, as previously described (14). Briefly, cancer and normal cells were washed with ice-cold PBS and were lysed with radioimmunoprecipitation assay buffer (Nacalai Tesque, Inc.) on ice for 15 min. Cell lysates were collected after centrifugation at 300 x g for 5 min at 4˚C, and the total protein concentration of the supernatant was determined spectrophotometrically using a NanoDrop 1000 spectrophotometer (NanoDrop; Thermo Fisher Scientific, Inc.). The supernatant from the cell lysate containing 100 μg of protein was incubated with 50 μl Protein G PLUS-agarose solution at 4˚C for 1 h, and following centrifugation at 19,000 x g for 3 min, the supernatant was transferred to a new tube. The supernatant was incubated at 4˚C for 1 h following addition of an anti-P5 antibody (1:100), and was further incubated at 4˚C overnight following the addition of 50 μl protein G PLUS-agarose solution. The agarose was collected by centrifugation at 19,000 x g for 3 min, washed at least three times with cold PBS, and boiled in SDS-PAGE sample buffer at 98˚C for 5 min. The samples were then separated by 12.5% SDS-PAGE, and the bound proteins were visualized by silver staining using Sil-Best Stain One (Nacalai Tesque, Inc.), according to the manufacturer's protocol. To examine the binding of vimentin with P5 in cells by immunoprecipitation, total cell lysates from U251, PE, BT20, H322, DLD-1, PA-1 and U937 cells were prepared, and immunoprecipitation was performed using the anti-P5 antibody as aforementioned. The samples were separated by 12.5% SDS-PAGE, and then western blotting was performed using anti-P5 and anti-vimentin antibodies.

Mass spectrometry and protein identification. The bands of interest were excised from the gel using a box cutter after silver staining, and in-gel digestion was performed using the In-gel tryptic digestion kit (Thermo Fisher Scientific, Inc.), according to the manufacturer's protocol. Gel trypsin digestion and protein identification by liquid chromatography-tandem mass spectrometry (LC/MS/MS) were performed as previously described (14) at the Medical Research Support Center, Kyoto University (Kyoto, Japan). Acquired datasets were analyzed using ProteinPilot Software v. 4.5 Beta (SCIEX, Tokyo, Japan) with the Paragon algorithm and a combined database of UniProtKB/Swiss-Prot data and known contaminants (SCIEX).

Biomolecular interactions. Surface plasmon resonance experiments were performed using the Biacore T100 system (GE Healthcare Bio-Sciences), as previously described (11). Briefly, recombinant human vimentin protein was immobilized on the surface of a CM5 sensor chip with *N*-hydroxysuccinimide and *N*-ethyl-*N*'-(dimethylaminopropyl) carbodiimide activation chemistry, according to the manufacturer's protocol. As an analyte, purified recombinant P5 protein was injected over the flow cell, and HBS-EP buffer (0.01 M HEPES, 0.15 M NaCl, 0.005% Tween-20, 3 mM EDTA, pH 7.4) was used as a running buffer to inhibit nonspecific binding. An approximate equilibrium dissociation constant (Kd) value was obtained as previously described using Biacore T100 evaluation software ver. 2.0.2 (GE Healthcare Bio-Sciences) (17).

RT-PCR. RT-PCR was performed as previously described (18). Briefly, following isolation of total RNA using a NucleoSpin RNA kit (MACHEREY-NAGEL GmbH & Co. KG, Düren, Germany), RT was conducted using a ReverTra Ace qPCR RT kit (Toyobo Life Science, Osaka, Japan), according to the manufacturer's protocol. Subsequently, each 1-μl aliquot of cDNA was amplified in a final 50-μl PCR mixture containing Titanium taq DNA Polymerase (1:100; Takara Bio, Inc., Otsu, Japan) and 0.2 mM dNTP mixture solution from the Long Range PCR kit (Qiagen GmbH, Hilden, Germany). The PCR thermocycling conditions were as follows: Initial denaturation at 94˚C for 1 min, followed by 30-35 cycles at 94˚C for 30 sec, 60-61˚C for 30 sec and 72˚C for 30 sec, and a final extension step at 72 ˚C for 30 sec. For upregulation of the CHOP gene, which is a positive control for ER stress, U251/Luc cells were treated with 0.5 μM Tg for 6 h at 37˚C, and cells were collected for the isolation of total RNA as aforementioned. Specific primers for RT-PCR were as follows: CCAAT-enhancer-binding protein homologous protein (CHOP), forward 5'-ATCAAAAATCTT CACCACTCTTGAC-3', reverse 5'-ACTTTCCTTTCATTC TCCTGTTCTT-3'; vimentin, forward 5'-GGTACAAATCCA AGTTTGCTGACC-3', reverse 5'-CTCAATGTCAAGGGC CATCTTAAC-3'; Snail, forward 5'-CAAGGCCATGTCCGG ACCCACACTGGCG-3', reverse 5'-CTTCCTGCTGGAGCT GGGGAAGGCTGTC-3'; Slug, forward 5'-GGCCAAACA TAAGCAGCTGCACTGCG-3', reverse 5'-CAGATGAGCCCT CAGATTTGACCTGTC-3'; Twist, forward 5'-GCAGACGCA GCGGGTCATGGCCAACG-3', reverse 5'-CATCCTCCA GACCGAGAAGGCGTAGC-3'; N-cadherin, forward 5'-GAC CCATCCACGCCGAGCCCCAGTATCCG-3', reverse 5'-CAC CCTGAAGTTCAGTCATCACCTCCACC-3'; E-cadherin, forward 5'-GCTAGTCTGAGCTCCCTGAACTCCTCA G-3', reverse 5'-GGGGCCCGCCTCTCTCGAGTCCCCTAG TCG-3'; and GAPDH, forward 5'-GTCTTCACCACCATG GAGAAGGCT-3' and reverse 5'-CATGCCAGTGAGCTT CCCGTTCA-3'. GAPDH was used as an internal control. PCR products were run on a 1% agarose gel, which was stained with GelRed (Biotium, Fremont, CA USA) for UV analysis.

Bioluminescence imaging. U251 cells stably transfected with pBipPro-Luc (U251/Luc), in which the Bip promoter region was cloned into the pGL4.14 vector (Promega Corporation), were prepared. Successful transfection was confirmed using the LV200 imaging system (Olympus Corporation, Tokyo, Japan), through the observation of bioluminescence, as previously described (19). Luminescence images at the single-cell level were obtained using the LV200 imaging system, as previously described (19). Briefly, 24 h post-transfection of U251/Luc cells with negative control or P5 siRNA, images were captured using a x40 objective lens at 10-min intervals, and Bip promoter activity was observed following the addition of D-luciferin. An expression vector of vimentin fused with PSmOrange (20) (vim/Orange) was provided by Addgene, Inc. (Cambridge, MA, USA). For the observation of vim/Orange, BP535-555HQ (Olympus Corporation) and 570-625RFP (Olympus Corporation) were used as excitation and emission filters, respectively. U251/Luc cells stably transfected with vim/Orange (U251/Luc/Orange) were also prepared in selective medium containing 200 μg/ml hygromycin B (Nacalai Tesque, Inc.) and 1,000 μg/ml G-418 (Wako Pure Chemical Industries, Ltd., Osaka, Japan). Successful transfection was confirmed using the LV200 system, through the observation of both bioluminescence and fluorescence using the filters. After the establishment of stable U251/Luc and U251/Luc/Orange cells, they were transfected with the negative control and P5 siRNAs, as aforementioned. All data analysis was performed using AQUACOSMOS ver. 2.6 software (Hamamatsu Photonics, Hamamatsu, Japan).

Statistical analysis. Experiments were repeated at least two times. Statistical significance was determined using Student's t-test for pairwise comparisons, whereas multiple comparisons were evaluated by one-way analysis of variance followed by Dunnett's test using JMP Pro version 14 (SAS Institute, Inc., Cary, NC, USA). $P<0.05$ was considered to indicate a statistically significant difference.

Results

Expression levels of P5 on the surface of normal and cancer cells. The present study examined the expression levels of P5 on the surface of normal and cancer cells by fluorescence-activated cell sorting (FACS) analysis using an affinity-purified anti-P5 antibody labeled with FAM-X, which was confirmed to be specific to P5 protein and did not cross-react with PDI or bovine serum albumin (Fig. 1A). The expression levels of P5 were detected on the cell lines shown in Table I using FACS analysis; the results revealed that P5 expression was markedly increased on the surface of several cancer cell lines, including U251, T98G, H322, DLD-1, HCT116, SW837, PA-1, U937, K562 and THP-1 cells compared with normal cell lines, and

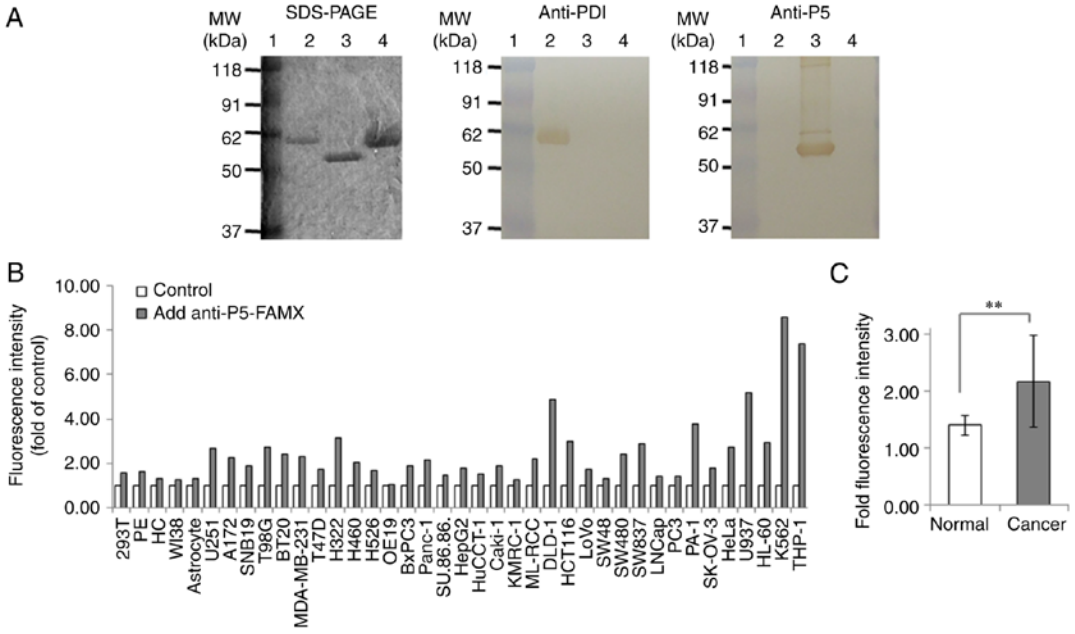

Figure 1. Expression levels of P5 on the surface of normal and cancer cells. (A) Specificity of the affinity-purified rabbit anti-P5 antibody. All proteins were separated by SDS-PAGE. Western blotting was performed using a rabbit anti-PDI raised against purified bovine PDI or affinity-purified anti-P5 antibody. Lane 1, prestained marker proteins; lane 2, purified PDI protein; lane 3, purified recombinant P5 protein from *Escherichia coli*; lane 4, bovine serum albumin. (B) Expression levels of P5 on the surface of normal and cancer cells, as determined by fluorescence-activated cell sorting analysis using an affinity-purified anti-P5 antibody labeled with FAM-X. The control group was not incubated with anti-P5, and was set at 1.0 for all cell lines. The assay was repeated two times to confirm the results. Data were not subjected to statistical analysis. (C) Fold fluorescence intensity of anti-P5 staining on the surface of normal cell lines compared with cancer cell lines, with the exception of the leukemia cell lines (U937, HL-60, K562 and THP-1). Data are presented as the means ± standard deviation. **P<0.01. FAM-X, 6-(fluorescein-5-carboxamido) hexanoic acid succinimidyl ester; HC, hepatocytes; PDI, protein disulfide isomerase; PE, pancreatic epithelial cells.

it was expressed at the highest levels on the surface of K562 and THP-1 cells, which are chronic myelogenous and acute monocytic leukemia cell lines (21,22), respectively (Fig. 1B). A constant increase in the surface expression of P5 was observed in glioblastoma (U251, A172, SNB19, and T98G), breast (BT20, MDA-MB-231, T47D), colon (DLD-1, HCT116, LOVO, SW480, SW837), and ovarian and uterine cervical (PA-1, SK-OV-3, HeLa) cancer, and leukemia (U937, HL-60, K562, THP-1) cell lines (Fig. 1B). In addition, the expression levels of P5 were compared between normal and cancer cell lines; its expression was significantly increased on the surface of cancer cell lines, compared with normal cells; leukemia cell lines were not included in this analysis (Fig. 1C). The present study also investigated the expression of P5 in these cell lines by western blotting using an anti-P5 antibody. P5 was expressed in all cell lines examined; however, its expression levels differed among the cell lines (Fig. 2A and B). When the expression levels of P5 in total cell lysates were compared between normal and cancer cell lines, it was revealed that its expression was not significantly different between normal and cancer cells; leukemia cell lines were not included in this analysis (Fig. 2B). These results suggested that P5 expression may be increased on the surface of several cancer cells compared with normal cells; however, the enzyme was expressed at a constant level within both normal and cancer cells.

Effects of P5 knockdown in cancer cells on activation of the Bip promoter during cancer cell growth. Alongside a previous report regarding the role of P5 in cancer cells (4), the present study indicated that P5 may have a significant role in cancer cells. Therefore, the present study further investigated the functional roles of P5 in cancer cells. The effects of P5 knockdown in cancer cells on activation of the Bip promoter during cancer cell growth were analyzed, as our previous study indicated that the Bip promoter is periodically activated, according to real-time monitoring using bioluminescence at the single-cell level in U251 glioblastoma cells (19). Following siRNA-induced knockdown of P5, western blotting confirmed that its expression was reduced in cancer cells (Fig. 3A). Real-time bioluminescence monitoring at the single-cell level demonstrated that Bip promoter activation was observed in U251/Luc cells even post-transfection with negative control siRNA during cancer cell growth (Fig. 3B and C), as shown in our previous study (19); however, it was not activated post-transfection with P5 siRNA, although Bip promoter activity was maintained and luminescence was still observed in the cancer cells (Fig. 3B and C). Since the Bip promoter is periodically activated, particularly in dividing cells during cell growth (19), these results suggested that knocking down P5 in cancer cells may affect Bip promoter activity and cancer cell division during cell growth. The present study investigated the effects of P5 knockdown in U251/Luc cells on the expression of Bip and CHOP, which are markers of ER stress responses; there was no significant difference in their expression between the groups transfected with the negative control or P5 siRNAs (Fig. 3D). Therefore, knocking down P5 in cancer cells may not induce an ER stress response.

Effects of P5 knockdown in cancer cells on cell growth and migration. Since Bip promoter activation during cancer cell

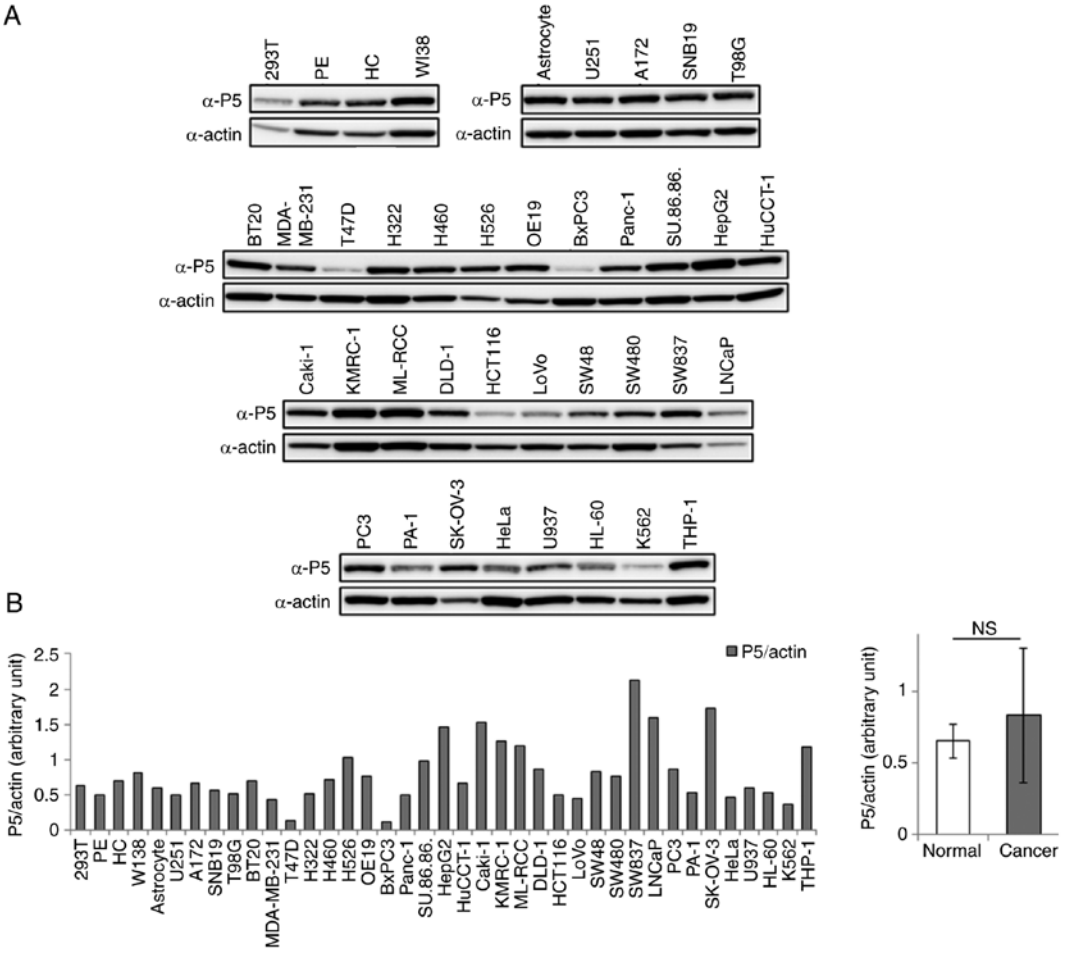

Figure 2. Western blot analysis of P5 protein in normal and cancer cells. (A) Western blotting of P5 in normal and cancer cell lines. Total protein extracts from normal and cancer cell lines were analyzed by western blotting using an α-P5 or α-actin antibody. β-actin was used as the loading control. (B) Expression levels of P5 protein in normal and cancer cell lines. Expression levels were calculated (left panel), and the expression levels were compared between the normal cell lines and cancer cell lines (leukemia cell lines, U937, HL-60, K562 and THP-1, were not included in this analysis). Data are presented as the means ± standard deviation. α, anti; HC, hepatocytes; n.s., not significant; PE, pancreatic epithelial cells.

growth was not observed post-transfection with P5 siRNA, the present study examined the effects of siRNA-induced P5 knockdown in U251/Luc cancer cells on cell growth and migration. P5 knockdown in cancer cells significantly inhibited cell growth, as assessed using the WST-8 assay, compared with in cells transfected with or without negative control siRNA (Fig. 4A); this phenomenon was also observed when using another glioblastoma cell line, SNB19 (data not shown). However, transfection of normal PE or astrocyte cells with P5 siRNA, in which the knockdown of P5 expression was confirmed by western blotting, did not inhibit cell growth (Fig. 4A). The present study also investigated the effects of P5 knockdown in U251/Luc cancer cells on cell migration; P5 knockdown reduced cancer cell migration compared with in cells transfected with or without negative control siRNA (Fig. 4B). These results suggested that P5 may serve an important role in cancer cell growth and migration.

Identification of a P5-binding protein in cancer cells. Since the present findings suggested that P5 serves important roles in cancer cells, further functional analysis of this enzyme was conducted by screening for specific proteins that bind to P5 in cancer cells compared with normal cells. Immunoprecipitation was performed using an anti-P5 antibody, and several proteins were revealed to specifically bind to P5 in cancer cells compared with normal cells (Fig. 5A). After performing the immunoprecipitation experiments several times, one of the protein bands visualized by SDS-PAGE and silver staining was identified as a specific protein that bound to P5 in cancer cells (Fig. 5A). To identify this binding protein, the band was excised from the gel, in-gel digested and analyzed by LC-MS/MS. The band was identified as human vimentin protein (data not shown). Subsequently, immunoprecipitation with an anti-P5 antibody using a total cell lysate from U251 cells, and western blotting using an anti-vimentin antibody, confirmed that vimentin could bind to P5. In addition, vimentin was revealed to bind to P5 predominantly in U251 glioblastoma cells (Fig. 5B). Subsequently, the present study performed a biomolecular interaction analysis with purified recombinant P5 and vimentin proteins using the Biacore T100 system; vimentin immobilized on the sensor chip was revealed to interact with P5 protein and the Kd value of this interaction was $1.13\pm0.26\times10^{-5}$ M (Fig. 5C). These results suggested that vimentin may bind to P5 specifically and is a P5-binding protein predominantly in glioblastoma cells.

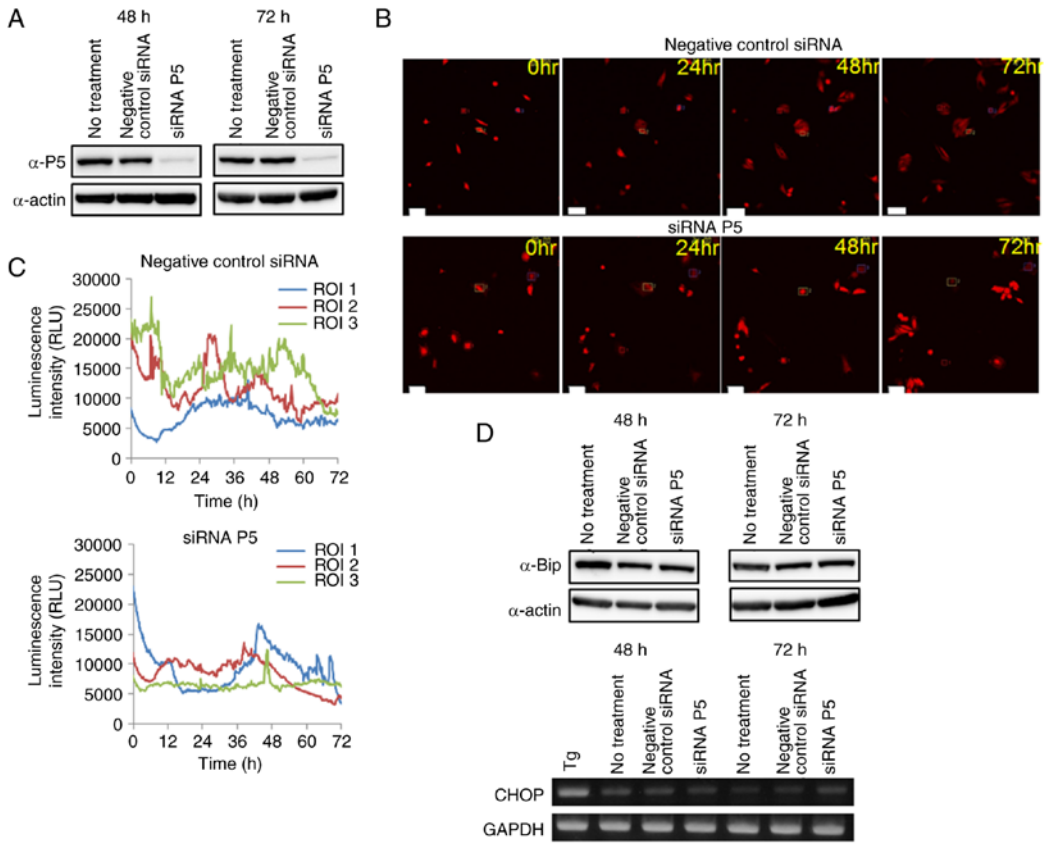

Figure 3. Effects of siRNA-induced P5 knockdown in cancer cells on activation of the Bip promoter. (A) Expression levels of P5 following siRNA transfection. U251/Luc cells were transfected with or without negative control or P5 siRNAs, and at 48 and 72 h post-transfection, the expression levels of P5 were detected by western blotting. β-actin was used as the loading control. (B) Luminescence images of U251/Luc cells transfected with negative control or P5 siRNAs obtained by the LV200 system at 0, 24, 48 and 72 h. Squares in the luminescence images indicate ROIs, in which luminescence intensity was measured for time-lapse analysis at the single-cell level. Scale bars, 100 μm. (C) Time course analysis of Bip promoter activation on single-cell level imaging. Time course analysis of Bip promoter activation in U251/Luc cells post-transfection with negative control or P5 siRNAs was performed using the LV200 system. (D) Effects of siRNA-induced P5 knockdown on the expression of Bip and CHOP. Upper panels, U251/Luc cells were transfected with or without negative control or P5 siRNAs, and at 48 and 72 h post-transfection, the protein expression levels of Bip protein were detected by western blotting. β-actin was used as the loading control. Lower panels, U251/Luc cells were transfected with or without negative control or P5 siRNAs, and at 48 and 72 h post-transfection, total RNA was extracted from these cells and reverse transcription-polymerase chain reaction was conducted. Treatment of U251/Luc cells with 0.5 μM Tg for 6 h was used as a positive control for upregulation of CHOP expression. α, anti; CHOP, CCAAT-enhancer-binding protein homologous protein; RLU, relative luminescence unit; ROI, region of interest; siRNA, small interfering RNA; Tg, thapsigargin.

Effects of knocking down P5 in cancer cells on cell morphology and EMT marker proteins. Since vimentin was revealed to predominantly bind to P5 in glioblastoma cells, the present study examined the effects of siRNA-induced P5 knockdown on the expression of vimentin in glioblastoma cells. P5 knockdown did not affect the expression of vimentin, as assessed by RT-PCR (Fig. 6A). Conversely, P5 knockdown affected the morphology of glioblastoma cells compared with cells transfected with negative control siRNA (Fig. 6B). The present study also conducted real-time monitoring, and simultaneously observed luminescence and fluorescence at the single-cell level using U251/Luc/Orange cells and the LV200 system; activity of the Bip promoter was decreased in cancer cells transfected with P5 siRNA and the expression pattern of vimentin was different from that in cells transfected with negative control siRNA (Fig. 6C). In addition, P5 knockdown inhibited the division of glioblastoma cells and induced death of cells that could not divide, as observed by the LV200 system (data not shown). These results suggested that P5 serves important roles in the division of glioblastoma cells and the localization of vimentin in these cells. Since vimentin is well known as a member of the intermediate filament family (23), and is widely used as a marker of EMT, which occurs during the metastasis of cancer cells (24,25), the effects of siRNA-induced P5 knockdown in glioblastoma cells on the expression of EMT marker proteins, such as Snail, Slug, Twist, N-cadherin and E-cadherin, were determined. P5 knockdown in glioblastoma cells decreased the expression of Snail and increased the expression of Slug; however, it had no effect on the expression of Twist, N-cadherin and E-cadherin, as assessed by RT-PCR (Fig. 6D).

Effects of anacardic acid and ribostamycin on the cytotoxic activity of TMZ against glioblastoma cells. The present study investigated the effects of anacardic acid on the cytotoxic activity of TMZ, in order to evaluate the availability of P5 for molecular targeting. In response to anacardic acid, the cytotoxic activity of TMZ against glioblastoma cells was not significantly affected (Fig. 7). However, a slight increase in the cytotoxic activity of TMZ was detected in the presence of both anacardic acid and ribostamycin; however, this finding was still not significant (Fig. 7).

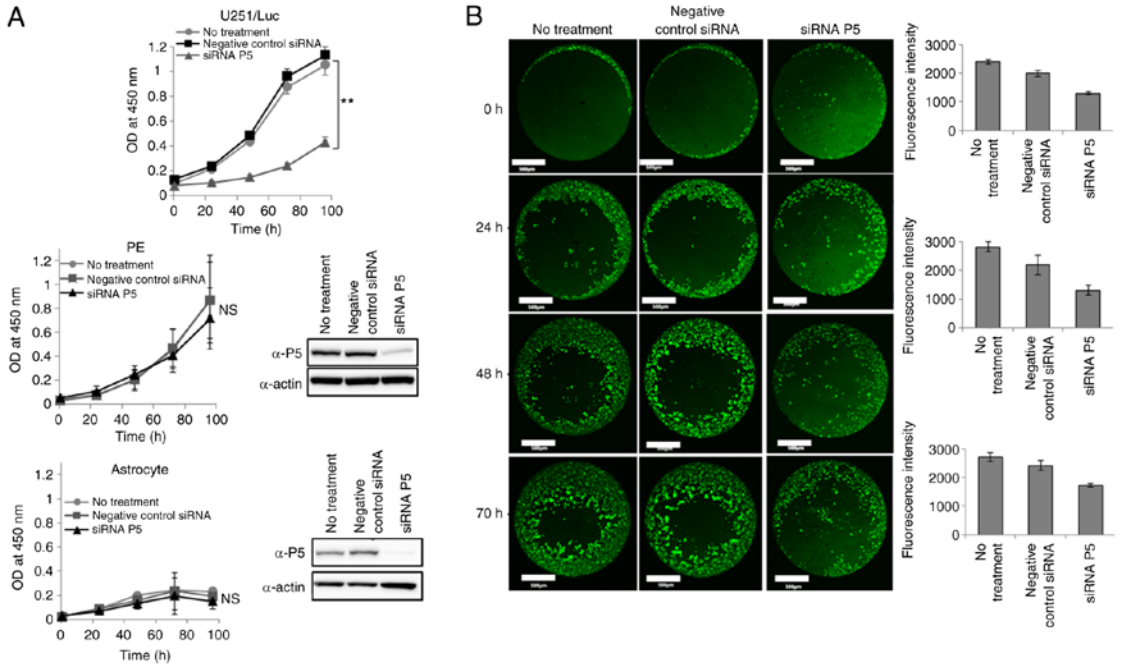

Figure 4. Effects of siRNA-induced P5 knockdown on cancer and normal cell growth, and cancer cell migration. (A) Effects of P5 knockdown on cancer (upper graph) and normal (middle and lower graphs) cell growth. U251/Luc cells, and normal PE cells and astrocytes were transfected with or without negative control or P5 siRNAs; 72 h post-transfection, cell growth was monitored using the WST-8 assay. Data are presented as the means ± SD from three independent experiments, and each assay was performed in triplicate. **P<0.01. Inset blots indicate the expression of P5 in PE cells or astrocytes 72 h post-transfection with siRNA. (B) Effects of P5 knockdown on cancer cell migration. U251/Luc cells were transfected with or without negative control or P5 siRNAs; 72 h post-transfection, the cells were seeded onto a 96-well migration assay plate and cell migration was assessed by confocal microscopy (left images) and a fluorescence microplate reader (right graphs), after staining with cell tracker green at the indicated time points. Data are presented as the means ± standard deviation of technical 8 replicate wells on a 96-well plate, and the assay was repeated two times to confirm the results. Data were not subjected to statistical analysis. Scale bars, 500 μm. α, anti; n.s., not significant; OD, optical density; siRNA, small interfering RNA.

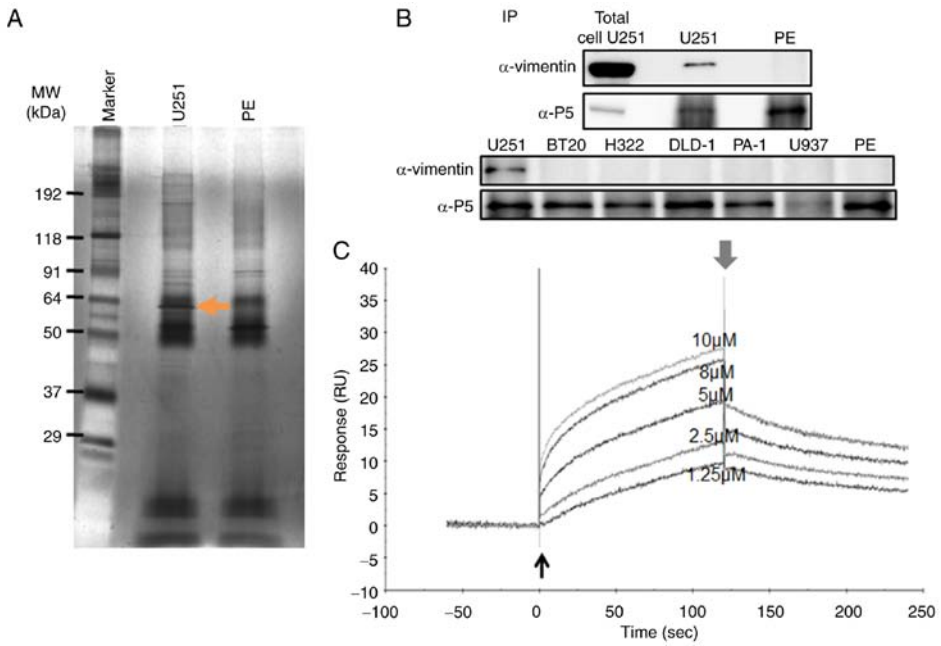

Figure 5. Isolation and identification of a specific P5-binding protein in cancer cells. (A) Immunoprecipitation of proteins associated with P5 in cancer and normal cells. Whole cell lysates were prepared from normal (PE) and cancer (U251) cells, and associated proteins were immunoprecipitated using an α-P5 antibody. Following SDS-PAGE for the separation of proteins bound to P5, silver staining was performed to visualize these proteins. The arrow indicates a P5-binding protein predominantly detected in cancer cells, which was identified by liquid chromatography-tandem mass spectrometry. (B) Immunoprecipitation of P5 with vimentin. Whole cell lysates from U251 and PE cells were prepared, and associated proteins were captured using protein G agarose resin. Vimentin was detected by western blotting using an α-vimentin antibody. Total cell U251 indicates the positive control for the detection of vimentin and P5, in which 30 μg protein from whole U251 cell lysates was loaded onto SDS-PAGE without immunoprecipitation, and detected with α-vimentin and α-P5 antibodies (upper panel). Whole cell lysates from U251, BT20, H322, DLD-1, PA-1, U937 and PE cells were also immunoprecipitated using an α-P5 antibody, and western blotting was performed for the detection of vimentin (lower panel). Detection of P5 in western blotting was performed as a control for immunoprecipitation. PE, pancreatic epithelial. (C) Sensorgrams of the binding of P5 protein to immobilized vimentin as determined by biosensor analysis. Recombinant vimentin protein was immobilized on the surface of sensor chips, and Purified human P5 protein was injected at various concentrations. Thin and thick arrows indicate the beginning and end of sample injection, respectively. α, anti.

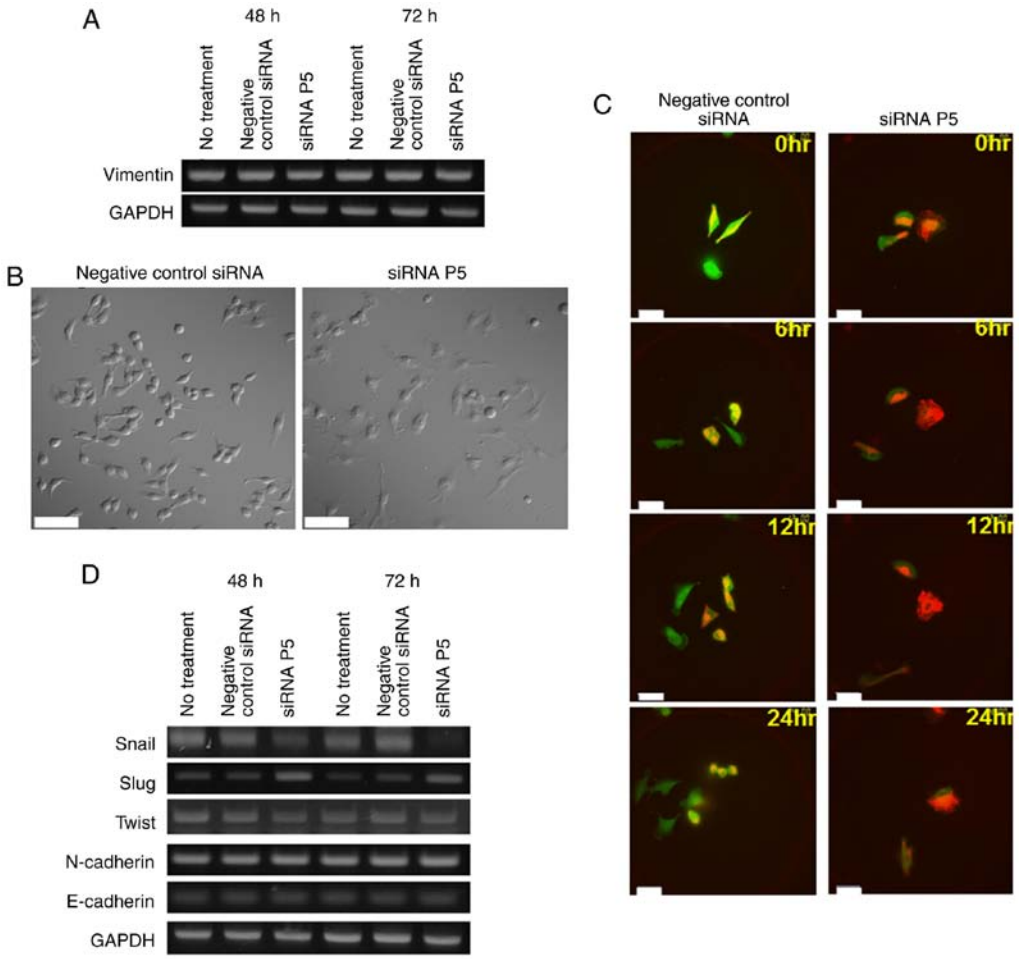

Figure 6. Effects of P5 knockdown on the expression of vimentin and EMT marker proteins in cancer cells. (A) Effect of siRNA-induced P5 knockdown on the expression of vimentin in cancer cells. U251/Luc cells were transfected with or without negative control or P5 siRNAs, and at 48 or 72 h post-transfection, total RNA was extracted from the cells and RT-PCR was performed. (B) Effects of siRNA-induced P5 knockdown on cancer cell morphology. U251/Luc cells were transfected with negative control or P5 siRNAs, and 48 h post-transfection, differential interference contrast images were obtained using an Olympus FV1000 confocal laser scanning microscope with x32 objective lens. Scale bars, 100 μm. (C) Images of real-time monitoring by simultaneous observation of bioluminescence and fluorescence. U251/Luc/Orange cells were transfected with negative control or P5 siRNAs, and at 48 h post-transfection, real-time monitoring of activity of the Bip promoter and the expression pattern of vimentin in cancer cells was performed by simultaneous observation of bioluminescence and fluorescence at the single-cell level using the LV200 system with a high magnification lens (x100). Green and orange in the images indicate Luc (bioluminescence) and Orange (fluorescence), respectively. Scale bars, 50 μm. (D) Effects of siRNA-induced P5 knockdown on the expression of EMT markers. U251/Luc cells were transfected with or without negative control or P5 siRNAs, and at 48 or 72 h post-transfection, total RNA was extracted from these cells. Reverse transcription-polymerase chain reaction for Snail, Slug, Twist, N-cadherin and E-cadherin was then performed. GAPDH was used as an internal control. At least three independent transfections were performed and confirmed in all assays. EMT, epithelial-mesenchymal transition; siRNA, small interfering RNA.

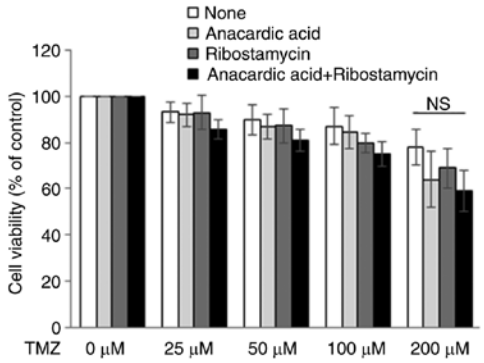

Figure 7. Effects of anacardic acid or ribostamycin on the cytotoxic activity of TMZ against cancer cells. U251/Luc cells were treated with or without TMZ at the indicated concentrations for 48 h in the presence or absence of anacardic acid (25 μM), ribostamycin (1 mM), or a combination of these compounds, and cell viability was analyzed. Data are expressed as the means ± standard deviation from three independent experiments and each assay was performed in triplicate. n.s., not significant; TMZ, temozolomide.

Discussion

The present study examined the expression levels of P5 on the surface of several normal and cancer cell lines, and demonstrated that its expression was increased in numerous cancer cell lines compared with normal cell lines. However, the expression of P5 in cell lysates, as assessed by western blotting, did not significantly differ between normal and cancer cells. Taken together with a previous report by Kaiser *et al*, in which P5 was suggested to serve significant roles in the secretion of soluble MICA from the surface of cancer cells (4), these results indicated that P5 on the surface of cancer cells may be a novel anticancer target.

Glioblastoma is the most common and aggressive malignancy of the central nervous system, and its prognosis remains dismal, despite recent developments in its treatment (26). Therefore, the identification and functional analysis of novel

candidate targets in glioblastoma cells will be indispensable for the improvement of chemotherapy. Since the expression levels of P5 on the surface of glioblastoma cells were increased compared with normal cell lines; however, marked differences in expression were not observed among these glioblastoma cell lines. Therefore, it was suggested that the expression levels of P5 would be constantly increased on the surface of glioblastoma, thus the present study focused on the functional analysis of P5 in glioblastoma cells. Among the glioblastoma cell lines used in this study, U251 cells are commonly used as experimental models of glioblastoma, and there are many reports and publications using this cell line. In addition, we previously reported that the transfection efficiency of plasmid DNA into U251 was sufficiently successful among the cell lines analyzed (27), suggesting that U251 cells may be used for experiments that introduce target genes into cells via plasmid DNA to establish a stable cell line, or for knockdown of genes with siRNA. The present study successfully established U251 cell lines stably transfected with a reporter vector, in which the Bip promoter region was cloned into a pGL4.14 vector for detection by reporter assay and bioluminescence imaging using the LV200 system; our previous study also reported that this cell line was available for the evaluation of chemical chaperones by real-time bioluminescence imaging (19). The present study used U251 and U251/Luc cells for functional analysis of P5, including bioluminescence imaging at the single-cell level. Although P5 has an ER retention signal sequence (Lys-Asp-Glu-Leu) at its C-terminus, several reports have demonstrated that PDI family proteins, including P5, localize not only to the ER but also to the nucleolus (28), cell surface (4,29,30), and mitochondria (5,6). It was recently reported that Bip (78-kDa glucose-regulated protein), which also has an ER retention signal sequence at its C-terminus, mainly exists as a peripheral protein on the plasma membrane of stressed cancer cells through its interaction with other cell surface proteins, such as glycosylphosphatidylinositol-anchored proteins, and that Bip expression on the cell surface requires its substrate-binding activity (31). Since several types of cancer cells activate numerous signal transduction pathways during the ER stress response to maintain ER homeostasis (32), and P5 also possesses chaperone activity, it has been suggested that P5 may be translocated to the surface of stressed cancer cells via a mechanism similar to that of Bip, by its substrate-binding site.

It has recently been reported that Bip has a key role as a prosurvival component in cancer cells, which can provide protection from cell death (33). In addition, it has been hypothesized that Bip is a novel target for increasing chemosensitivity in malignant gliomas (34). On the basis of these reports, our previous study performed real-time monitoring of Bip promoter activity during U251 glioblastoma cell growth using a bioluminescence imaging technique at the single-cell level, and reported how such bioluminescence imaging techniques could be used to analyze real-time promoter activity (19). In addition, it has been reported that P5 forms a noncovalent complex with Bip and cooperates with the chaperone protein toward client proteins (35). Taken together with these previous reports and observations, the present study investigated the effects of P5 knockdown in U251 glioblastoma cells on Bip promoter activation by bioluminescence imaging at the single-cell level; the results revealed that activation of the Bip promoter during cancer cell growth was affected by transfection with P5 siRNA compared with negative control siRNA. P5 knockdown in glioblastoma cells also inhibited cell growth and migration, although it did not affect the growth of normal PE cells and astrocytes. Therefore, it has been suggested that P5 may serve an important role in the growth of glioblastoma cells. Since Bip knockdown in glioblastoma cells also induces the ER stress response, as determined by CHOP upregulation following Bip knockdown (34), the present study examined the effects of siRNA-induced P5 knockdown on the expression levels of Bip and CHOP, and revealed that it had no effect on their expression. Therefore, knocking down P5 in cancer cells may not induce the ER stress response; this phenomenon may be considered another advantage for targeting P5 in glioblastoma cells, which operates via a mechanism different from that of Bip knockdown, since the ER stress response in cancer can also increase cell survival and protect against cell death (33).

To further elucidate the functional roles of P5 in glioblastoma cells, the present study screened for specific P5-binding proteins in glioblastoma cells compared with in normal cells, and successfully identified vimentin as a P5-binding protein in glioblastoma cells. Vimentin is a well-known member of the intermediate filament family (23), and it has been reported that vimentin induces cell shape alterations during EMT (24). Notably, P5 knockdown induced a morphological alteration in glioblastoma cells and affected the expression of EMT markers Snail and Slug; however, it did not affect the expression of Twist, N-cadherin and E-cadherin. Since vimentin did not bind to P5 in normal cells, and P5 knockdown did not affect normal cell growth, these results suggested that P5 may participate in the stabilization or regulation of vimentin via protein-protein interactions, and in EMT homeostasis, in glioblastoma cells. Further investigations are required to validate this hypothesis. Since Snail has an oncogenic role in glioblastoma by promoting EMT (25) and P5 knockdown in glioblastoma cells reduced the expression of Snail, targeting P5 in glioblastoma cells may also increase the efficacy of treatment for this malignancy.

The present study demonstrated that simultaneous real-time monitoring of bioluminescence and fluorescence at the single-cell level using the LV200 system could provide useful information about the effects of P5 knockdown in glioblastoma cells on Bip promoter activity and the expression pattern of vimentin. Bioluminescence imaging has several advantages, such as low background and high quantification (36), which are necessary for the analysis of promoter activity with a reporter gene; the avoidance of low levels of damage to living cells from excitation illumination (37); and longer available observation periods (38). Fluorescence imaging also has advantages for time-lapse imaging, such as the observation of expression patterns and localization of proteins in cells, in which it is possible to obtain clear images compared with bioluminescence even with short observation periods. Therefore, the method of simultaneous observation of fluorescence and bioluminescence at the single-cell level described in the present study may be considered a novel and attractive approach for the functional analysis of promoter activity and protein localization in various cells, including cancer cells.

The present study also investigated the effects of anacardic acid, which was previously identified as an inhibitor of the reductase activity of P5 (11), on the cytotoxic activity of TMZ, which is used clinically for the treatment of glioblastoma (39), in order to evaluate the availability of P5 for molecular targeting. In response to anacardic acid, the cytotoxic activity of TMZ against glioblastoma cells was not affected; however, the cytotoxic activity of TMZ was slightly increased in the presence of anacardic acid and ribostamycin; ribostamycin was previously revealed to inhibit the chaperone activity of PDI in cells (40). Although these findings were not significantly different, these results suggested that inhibitors of both the isomerase and chaperone activities of P5 may be suitable drugs for the effective enhancement of chemotherapy against glioblastoma, although further study of P5 in glioblastoma cells is required to support this suggestion. Therefore, P5 may be considered a novel, attractive and potent target for the treatment of glioblastoma.

In conclusion, to the best of our knowledge, this is the first study to report that one of the proteins that binds to P5 in U251 glioblastoma cells is vimentin, and the present findings indicated that P5 may be an attractive target for novel molecular targeted therapy of glioblastoma. However, the results of P5 functional analyses in glioblastoma cells were obtained from limited cell lines, and further studies are required to confirm the detailed functional roles of P5 in glioblastoma cells. Taken together with previous research into the roles of vimentin and EMT in glioblastoma cells, these observations may be provide useful information for further studies into the mechanism underlying the functional roles of P5 in cancer cells, which might assist in the development of novel treatments for glioblastoma.

Acknowledgements

The authors would like to thank Dr Shinji Ito (Medical Research Support Center, Kyoto University) for providing assistance with mass spectrometry and protein identification; Ms. Mitsuko Tachi, Ms. Nanako Okushima and Ms. Aki Matsumoto for providing technical assistance with cell culturing (Department of Pharmacoepidemiology, Kyoto University); and Dr Thoru Komiya for providing the affinity-purified rabbit anti-P5 antibody. They would also like to thank Mr. Ryutaro Akiyoshi and Ms. Yoko Hatta-Ohashi (Olympus Corporation) for providing technical assistance and advice on bioluminescence imaging using the LV200 system.

Funding

The present study was supported by Grants-in-Aid for Young Scientists (B) (grant no. 26870287), Grants-in-Aid for Scientific Research (B) (grant no. 26290052) and Grants-in-Aid for Scientific Research (C) (grant no. 16K07170) from the Japan Society for the Promotion of Science. The present study was also supported in part by a collaboration research fund from Olympus Corporation.

Availability of data and materials

The datasets used and/or analyzed during the current study are available from the corresponding author on reasonable request.

Authors' contributions

TH and KK conceived the study, designed the experimental methods, and supervised the study. AT and YM performed the purification of recombinant proteins, FACS and western blot analysis. AT established the stable cell lines, and performed the cell migration assay and bioluminescence imaging using the LV200 system. TH and AT performed the rest of the experiments. TH, AT and KK contributed to the interpretation of the data. TH wrote the manuscript, and AT and KK reviewed and edited the manuscript. All authors read and approved the final manuscript.

Ethics approval and consent to participate

Not applicable.

Patient consent for publication

Not applicable.

Competing interests

Koji Kawakami serves as a scientific advisor to Olympus Corporation. None of the other authors have any potential competing interests.

References

1. Laurindo FR, Pescatore LA and Fernandes Dde C: Protein disulfide isomerase in redox cell signaling and homeostasis. Free Radic Biol Med 52: 1954-1969, 2012.
2. Galligan JJ and Petersen DR: The human protein disulfide isomerase gene family. Hum Genomics 6: 6, 2012.
3. Kikuchi M, Doi E, Tsujimoto I, Horibe T and Tsujimoto Y: Functional analysis of P5, a protein disulfide isomerase homologue. J Biochem 132: 451-455, 2002.
4. Kaiser BK, Yim D, Chow IT, Gonzalez S, Dai Z, Mann HH, Strong RK, Groh V and Spies T: Disulphide-isomerase-enabled shedding of tumor-associated NKG2D ligands. Nature 447: 482-486, 2007.
5. Kimura T, Horibe T, Sakamoto C, Shitara Y, Fujiwara F, Komiya T, Yamamoto A, Hayano T, Takahashi N and Kikuchi M: Evidence for mitochondrial localization of P5, a member of the protein disulphide isomerase family. J Biochem 144: 187-196, 2008.
6. Shitara Y, Tonohora Y, Goto T, Yamada Y, Miki T, Makino H, Miwa M and Komiya T: Mitochondrial P5, a member of protein disulphide isomerase family, suppresses oxidative stress-induced cell death. J Biochem 152: 73-85, 2012.
7. Lovat PE, Corazzari M, Armstrong JL, Martin S, Pagliarini V, Hill D, Brown AM, Piacentini M, Birch-Machin MA and Redfern CP: Increasing melanoma cell death using inhibitors of protein disulfide isomerases to abrogate survival response to endoplasmic reticulum stress. Cancer Res 68: 5363-5369, 2008.
8. Bonome T, Levine DA, Shih J, Randonovich M, Pise-Masison CA, Bogomolniy F, Ozbun L, Brady J, Barrett JC, Boyd J, *et al*: A gene signature predicting for survival in suboptimally debulked patients with ovarian cancer. Cancer Res 68: 5478-5486, 2008.
9. Talantov D, Mazumder A, Yu JX, Briggs T, Jiang Y, Backus J, Atkins D and Wang Y: Novel genes associated with malignant melanoma but not benign melanocytic lesions. Clin Cancer Res 11: 7234-7242, 2005.
10. Xu S, Butkevich AN, Yamada R, Zhou Y, Debnath B, Duncan R, Zandi E, Petasis NA and Neamati N: Discovery of an orally active small-molecule irreversible inhibitor of protein disulfide isomerase for ovarian cancer treatment. Proc Natl Acad Sci USA 109: 16348-16353, 2012.
11. Horibe T, Torisawa A, Okuno Y and Kawakami K: Discovery of protein disulfide isomerase P5 inhibitors that reduce the secretion of MICA from cancer cells. ChemBioChem 15: 1599-1606, 2014.

12. Kimura T, Nishida A, Ohara N, Yamagishi D, Horibe T and Kikuchi M: Functional analysis of the CXXC motif using phage antibodies that cross-react with protein disulphide-isomerase family proteins. Biochem J 382: 169-176, 2004.
13. Obiri NI, Hillman CG, Haas GP, Sud S and Puri RK: Expression of high affinity interleukin-4 receptors on human renal cell carcinoma cells and inhibition of tumor cell growth in vitro by interleukin-4. J Clin Invest 91: 88-93, 1993.
14. Kohno M, Horibe T, Ohara K, Ito S and Kawakami K: The membrane-lytic peptide K8L9 and melittin enter cancer cells via receptor endocytosis following subcytotoxic exposure. Chem Biol 21: 1522-1532, 2014.
15. Kohno M, Horibe T, Haramoto M, Yano Y, Ohara K, Nakajima O, Matsuzaki K and Kawakami K: A novel hybrid peptide targeting EGFR-expressing cancers. Eur J Cancer 47: 773-783, 2011.
16. Honjo Y, Horibe T, Torisawa A, Ito H, Nakanishi A, Mori H, Komiya T, Takahashi R and Kawakami K: Protein disulfide isomerase P5-immunopositive inclusions in patients with Alzheimer's disease. J Alzheimers Dis 38: 601-609, 2014.
17. MacLeod TJ, Kwon M, Filipenko NR and Waisman DM: Phospholipid-associated annexin A2-S100A10 heterotetramer and its subunits: Characterization of the interaction with tissue plasminogen activator, plasminogen, and plasmin. J Biol Chem 278: 25577-25584, 2003.
18. Yang L, Horibe T, Kohno M, Haramoto M, Ohara K and Kawakami K: Targeting interleukin-4 receptor α with hybrid peptide for effective cancer therapy. Mol Cancer Ther 11: 235-243, 2012.
19. Horibe T, Okushima N, Torisawa A, Akiyoshi R, Hatta-Ohashi Y, Suzuki H and Kawakami K: Evaluation of chemical chaperones based on the monitoring of Bip promoter activity and visualization of extracellular vesicles by real time bioluminescence imaging. Luminescence 33: 249-255, 2018.
20. Subach OM, Patterson GH, Ting LM, Wang Y, Condeelis JS and Verkhusha VV: A photoswitchable orange-to-far-red fluorescent protein, PSmOrange. Nat Methods 8: 771-777, 2011.
21. Lozzio CB and Lozzio BB: Human chronic myelogenous leukemia cell-line with positive Philadelphia chromosome. Blood 45: 321-334, 1975.
22. Tsuchiya S, Yamabe M, Yamaguchi Y, Kobayashi Y, Konno T and Tada K: Establishment and characterization of a human acute monocytic leukemia cell line (THP-1). Int J Cancer 26; 171-176, 1980.
23. Satelli A and Li S: Vimentin in cancer and its potential as a molecular target for cancer therapy. Cell Mol Life Sci 68: 3033-3046, 2011.
24. Mendez MG, Kojima S and Goldman RD: Vimentin induces changes in cell shape, motility, and adhesion during the epithelial to mesenchymal transition. FASEB J 24: 1838-1851, 2010.
25. Myung JK, Choi SA, Kim SK, Wang KC and Park SH: Snail plays an oncogenic role in glioblastoma by promoting epithelial mesenchymal transition. Int J Exp Pathol 7: 1977-1987, 2014.
26. Jhanwar-Uniyal M, Labagnara M, Friedman M, Kwasnicki A and Murali R: Glioblastoma: Molecular pathways, stem cells and therapeutic targets. Cancers 7: 538-555, 2015.
27. Horibe T, Torisawa A, Akiyoshi R, Hatta-Ohashi Y, Suzuki H and Kawakami K: Transfection efficiency of normal and cancer cell lines and monitoring of promoter activity by single-cell bioluminescence imaging. Luminescence 29: 96-100, 2014.
28. Turano C, Coppari S, Altieri F and Ferraro A: Proteins of the PDI family: Unpredicted non-ER locations and functions. J Cell Physiol 193: 154-163, 2002.
29. Barbouche R, Miquelis R, Jones IM and Fenouillet E: Protein-disulfide isomerase-mediated reduction of two disulfide bonds of HIV envelope glycoprotein 120 occurs post-CXCR4 binding and is required for fusion. J Biol Chem 278: 3131-3136, 2003.
30. Ryser HJ, Levy EM, Mandel R and DiSciullo GJ: Inhibition of human immunodeficiency virus infection by agents that interfere with thiol-disulfide interchange upon virus-receptor interaction. Proc Natl Acad Sci USA 91: 4559-4563, 1994.
31. Tsai YL, Zhang Y, Tseng CC, Stanciauskas R, Pinaud F and Lee AS: Characterization and mechanism of stress-induced translocation of 78-kilodalton glucose-regulated protein (GRP78) to the cell surface. J Biol Chem 290: 8049-8064, 2015.
32. Davenport EL, Morgan GJ and Davies FE: Untangling the unfolded protein response. Cell Cycle 7: 865-869, 2008.
33. Schönthal AH: Pharmacological targeting of endoplasmic reticulum stress signaling in cancer. Biochem Pharmacol 85: 653-666, 2013.
34. Pyrko P, Schönthal AH, Hofman FM, Chen TC and Lee AS: The unfolded protein response regulator GRP78/BiP as a novel target for increasing chemosensitivity in malignant gliomas. Cancer Res 67: 9809-9816, 2007.
35. Jessop CE, Watkins RH, Simmons JJ, Tasab M and Bulleid NJ: Protein disulfide isomerase family members show distinct substrate specificity: P5 is target to BiP client proteins. J Cell Sci 122: 4287-4295, 2009.
36. Choy G, O'Connor S, Diehn FE, Costouros N, Alexander HR, Choyke P and Libutti SK: Comparison of noninvasive fluorescent and bioluminescent small animal optical imaging. Biotechniques 35: 1022-1026, 2003.
37. Dixit R and Cyr R: Cell damage and reactive oxygen species production induced by fluorescence microscopy: Effect on mitosis and guidelines for non-invasive fluorescence microscopy. Plant J 36: 280-290, 2003.
38. Strayer C, Oyama T, Schultz TF, Raman R, Somers DE, Más P, Panda S, Kreps JA and Kay SA: Cloning of the *Arabidopsis* clock gene *TOC1*, an autoregulatory response regulator homolog. Science 289: 768-771, 2000.
39. Venur VA, Peereboom DM and Ahluwalia MS: Current medical treatment of glioblastoma. Cancer Treat Res 163: 103-115, 2015.
40. Ko MK and Kay EP: PDI-mediated ER retention and proteasomal degradation of procollagen I in corneal endothelial cells. Exp Cell Res 295: 25-35, 2004.